arXiv:1408.6060v1 [hep-ex] 26 Aug 2014

Proceedings of the Second Annual LHCP

August 27, 2014

New results in B decays

Mark Whitehead

On behalf of the LHCb collaboration,
Department of Physics
University of Warwick, Coventry, CV4 7AL, U.K.

ABSTRACT

The latest results from studies of b hadron decays to open charm final states at the LHCb experiment are presented. The results include measurements of CP violation and the properties of b baryons.

PRESENTED AT

The Second Annual Conference
on Large Hadron Collider Physics
Columbia University, New York, U.S.A
June 2-7, 2014

1 Introduction

Decays of beauty hadrons to open charm final states are an important part of the LHCb physics programme. A key goal is measuring the CKM angle γ, which is the least precisely measured angle of the unitarity triangle. Decays such as $B^- \to DK^-$, where D is D^0 or $\overline{D}^0$, are very important for measuring γ by exploiting the GLW [1, 2], ADS [3] and GGSZ [4] methods. In addition, measurements of the properties of beauty and charm hadrons can be made with excellent precision.

The LHCb detector [5] is a single arm spectrometer based at the Large Hadron Collider at CERN. The detector was optimised to study b and c hadron decays. Decays of b hadrons to open charm final states are predominantly selected by an efficient hadronic trigger. Described in this document are three analyses from LHCb, two of which use the full 3.0 fb^{-1} run one dataset and one uses 1.0 fb^{-1} of data collected in 2011.

2 Analysis of $B^- \to DK^-$ with $D \to K^0_S K^\mp \pi^\pm$

The decay $B^- \to DK^-$ with $D \to K^0_S K^\mp \pi^\pm$ provides an ADS-like approach to measure γ. Two categories can be defined by requiring that the charged kaons have the same sign (SS) or opposite sign (OS). A control channel $B^- \to D\pi^-$ with $D \to K^0_S K^\mp \pi^\pm$ is used, which is expected to have much smaller sensitivity to γ. Input from CLEO-c [6] is required to describe the variation of the strong phase and the coherence factor. These parameters are measured across the full Dalitz plot and in the $K^*(892)^\pm$ region, where the coherence factor and hence sensitivity to γ is expected to be larger.

The full 3.0 fb^{-1} data sample is exploited and the $K^0_S \to \pi^+\pi^-$ final state is used. A boosted decision tree (BDT) is used to discriminate between signal decays and combinatorial background. The BDT is trained using simulated signal events and a background sample from the high B mass sideband. Following the selection requirements a fit is performed to the B candidate invariant mass distribution. Signal peaks are parametrised with double Crystal Ball functions [7]. The combinatorial background is modelled with a linear function, the partially reconstructed background by a non-parametric function derived from $B^- \to D^0 h^-$ with $D^0 \to K^-\pi^+$ data, where h is a kaon or pion. Additionally, the fit to $B^- \to DK^-$ includes a cross-feed contribution from $B^- \to D\pi^-$ decays, modelled with a Crystal Ball function. An example of the B candidate

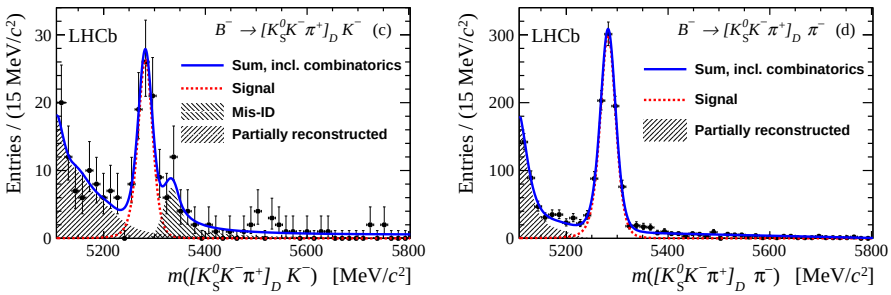

Figure 1: Fit to the SS B^- candidate invariant mass distribution for (left) $B^- \to DK^-$ and (Right) $B^- \to D\pi^-$ decays. The legend describes the fit components and the black points are the data.

invariant mass fit for the SS candidates is shown in Fig. 1. The signal yields for the various categories are summarised in Table. 1. These are used to calculate several observables (defined in Ref [8]), three of which are effectively yield ratios between categories ($\mathcal{R}$). The remaining four are charge asymmetries ($\mathcal{A}$) between B^+ and B^- decays. The results of these are given in Table 2, where corrections due to efficiency and production and detection asymmetries are applied. These observables are sensitive to both γ and r_B, where r_B is the ratio of the interfering $B^- \to DK^-$ amplitudes. Scans of the $\gamma - r_B$ parameter space is shown in Fig. 2, where the χ^2 probability is calculated at each point, taking into account statistical and systematic uncertainties. For comparison, the result of a previous LHCb γ combination [9] is shown as the black point. The results shown here are compatible with this and will help to improve future global fits of the angle γ.

Note that there is increased precision on γ in the $K^*(892)^\pm$ region, as expected. For more details on this analysis please see Ref. [8].

Table 1: Signal yields and statistical uncertainties from the B candidate invariant mass fit.

	Whole Dalitz plot		$K^*(892)^\pm$ region	
Mode	$DK^\pm$	$D\pi^\pm$	$DK^\pm$	$D\pi^\pm$
SS	145 ± 15	1841 ± 47	97 ± 12	1365 ± 38
OS	71 ± 10	1267 ± 37	26 ± 6	553 ± 24

Table 2: Value of the observables with statistical (first) and systematic (second) uncertainties.

Observable	Whole Dalitz plot	$K^*(892)^\pm$ region
$\mathcal{R}_{\rm SS/OS}$	$1.528 \pm 0.058 \pm 0.025$	$2.57 \pm 0.13 \pm 0.06$
$\mathcal{R}_{DK/D\pi,{\rm SS}}$	$0.092 \pm 0.009 \pm 0.004$	$0.048 \pm 0.011 \pm 0.003$
$\mathcal{R}_{DK/D\pi,{\rm OS}}$	$0.066 \pm 0.009 \pm 0.002$	$0.056 \pm 0.013 \pm 0.002$
$\mathcal{A}_{{\rm SS},DK}$	$0.040 \pm 0.091 \pm 0.018$	$0.026 \pm 0.109 \pm 0.029$
$\mathcal{A}_{{\rm OS},DK}$	$0.233 \pm 0.129 \pm 0.024$	$0.336 \pm 0.208 \pm 0.026$
$\mathcal{A}_{{\rm SS},D\pi}$	$-0.025 \pm 0.024 \pm 0.010$	$-0.012 \pm 0.028 \pm 0.010$
$\mathcal{A}_{{\rm OS},D\pi}$	$-0.052 \pm 0.029 \pm 0.017$	$-0.054 \pm 0.043 \pm 0.017$

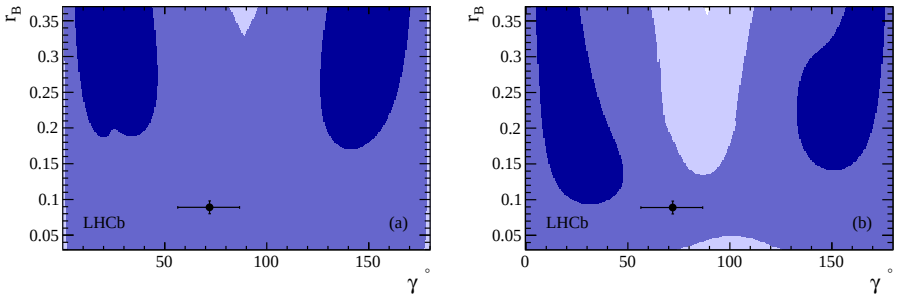

Figure 2: Two dimensional plot of γ against r_B for (left) the full Dalitz plot and (right) the $K^*(892)^0$ region. The contours show the (dark) $1\,\sigma$, (middle) $2\,\sigma$ and (light) $3\,\sigma$ of the χ^2 probability.

3 Model dependent GGSZ analysis of $B^- \to DK^-$ decays

The GGSZ method uses decays of the D meson to three-body quasi-self-conjugate final states such as $D \to K^0_{\rm S}\pi^-\pi^+$ to make a measurement of γ. In this model-dependent analysis [10] an amplitude model from BaBar [11] is used to perform a fit to the $D \to K^0_{\rm S}\pi^-\pi^+$ Dalitz plot. The decay $B^- \to D\pi^-$ with the same D decay is used as a control mode.

Candidates are selected using the $K^0_{\rm S} \to \pi^+\pi^-$ final state. The candidates are split into two categories depending on the K^0_S reconstruction, those with both daughters having hits in the vertex locator are known as long candidates and those without known as downstream candidates. Following selection requirements on kinematic variables, and some particle identification criteria, fits to the B candidate invariant mass distribution are performed. The mass fit is performed to determine signal and background yields which are used as an input to the Dalitz plot fit. The mass fits are performed simultaneously across the DK and $D\pi$ final states and long and downstream candidates are fitted separately. An example mass fit for long candidates in the DK final state is shown in Fig. 3 (left).

The fit to the D decay Dalitz plots are performed simultaneously across long and downstream candidates, DK and $D\pi$ final states and for B^+ and B^- candidates. The efficiency variation, modelled as a second-order

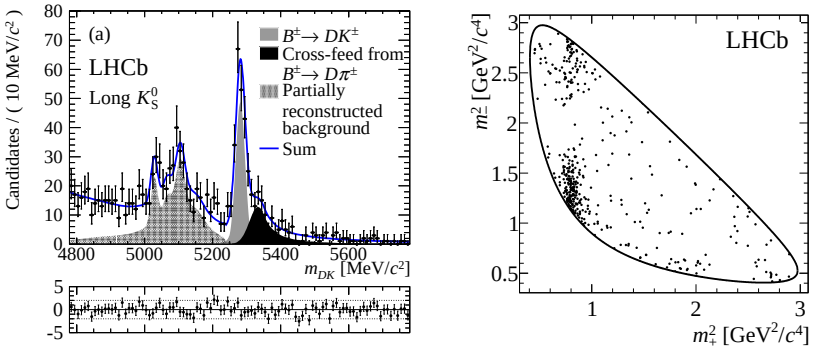

Figure 3: (Left) fit to the B candidate invariant mass distribution for long K^0_S candidates with a normalised residual plot and (right) the D Dalitz plot distribution of all B^+ candidates in the DK final state.

polynomial is determined using the $D\pi$ final state where the suppressed B decay is expected to be negligible. The Dalitz plot distribution of $D \to K^0_S\pi^+\pi^-$ candidates from the $B^+ \to DK^+$ decay is shown in Fig. 3 (right), where the $K^*(892)^+$ resonance is visible. The fits are used to extract parameters $x_\pm$ and $y_\pm$, defined in Ref. [10]. Projections of the Dalitz plot fit together with the data are shown in Fig. 4 for B^+ candidates in the DK decay mode, where $m_\pm = m_{K^0_S\pi^\pm}$ and $m_0 = m_{\pi^+\pi^-}$. The values of $x_\pm$ and $y_\pm$ derived from the fit are

$$\begin{aligned} x_- &= +0.027 \pm 0.044\,^{+0.010}_{-0.008} \pm 0.001, \\ y_- &= +0.013 \pm 0.048\,^{+0.009}_{-0.007} \pm 0.003, \\ x_+ &= -0.084 \pm 0.045 \pm 0.009 \pm 0.005, \\ y_+ &= -0.032 \pm 0.004\,^{+0.010}_{-0.009} \pm 0.008, \end{aligned}$$

where the uncertainties are statistical, systematic and from the amplitude model, respectively. From these quantities the values for the magnitude of the ratio of interfering $B^\pm$ amplitudes, the strong phase difference between them and γ are found to be $r_B = 0.06 \pm 0.04$, $\delta_B = (115^{+41}_{-51})^\circ$ and $\gamma = (84^{+49}_{-42})^\circ$. Neutral D meson mixing has a negligible effect on each of the determined parameters. These results are consistent with the model-independent analysis using the same data sample [12] and the world average values [13, 14]. For more details on this analysis please see Ref. [10].

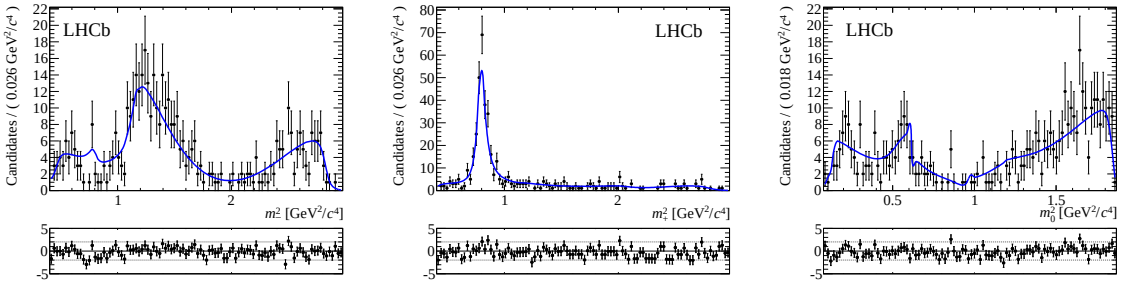

Figure 4: Projections of the Dalitz plot fit (blue) on to data (black) for (left) m^2_-, (middle) m^2_+ and (right) m^2_0.

4 Measurement of the mass and lifetime of the Ξ^0_b baryon

Large samples of b baryons are produced at the LHC, allowing for accurate measurements of their properties. Measurements of the mass and lifetime of the Ξ^0_b baryon, which has quark content bsu, are not very pre-

cise [15]. The analysis [16], based on the 3 fb^{-1} data sample, uses the $\Xi_b^0 \to \Xi_c^+\pi^-$ decay with $\Xi_c^+ \to pK^-\pi^+$ and the normalisation decay mode is $\Lambda_b^0 \to \Lambda_c^+\pi^-$ with $\Lambda_c^+ \to pK^-\pi^+$.

A BDT is used to separate signal decays from combinatorial background and is trained using signal decays from simulation and background from the high b baryon mass sideband. A fit is performed to the b baryon candidate invariant mass distribution to extract the signal yields. The fit is performed simultaneously to samples of Λ_b^0 and Ξ_b^0 candidates. The invariant masses of charm baryon candidates are also fitted, to enable a mass measurement of the Ξ_c^0 baryon. Signals are modelled with double Crystal Ball functions, misidentified backgrounds are fitted with non-parametric shapes determined from simulation, an exponential shape is used for the combinatorial background and partially reconstructed decays are modelled by an ARGUS function [17] convolved with a Gaussian. The fits are shown in Fig. 5 for both Λ_b^0 and Ξ_b^0 candidates. The mass differences between the two b baryons and the two c baryons are determined to be

$$\begin{aligned} M(\Xi_b^0) - M(\Lambda_b^0) &= 172.44 \pm 0.39(\text{stat}) \pm 0.17(\text{syst})\,\text{MeV}/c^2, \\ M(\Xi_c^+) - M(\Lambda_c^+) &= 181.51 \pm 0.14(\text{stat}) \pm 0.10(\text{syst})\,\text{MeV}/c^2. \end{aligned}$$

Using the world average values for $M(\Lambda_b^0)$ and $M(\Lambda_c^+)$ these become

$$\begin{aligned} M(\Xi_b^0) &= 5791.80 \pm 0.39(\text{stat}) \pm 0.17(\text{syst}) \pm 0.26(M(\Lambda_b^0))\,\text{MeV}/c^2, \\ M(\Xi_c^+) &= 2467.97 \pm 0.14(\text{stat}) \pm 0.10(\text{syst}) \pm 0.14(M(\Lambda_c^+))\,\text{MeV}/c^2. \end{aligned}$$

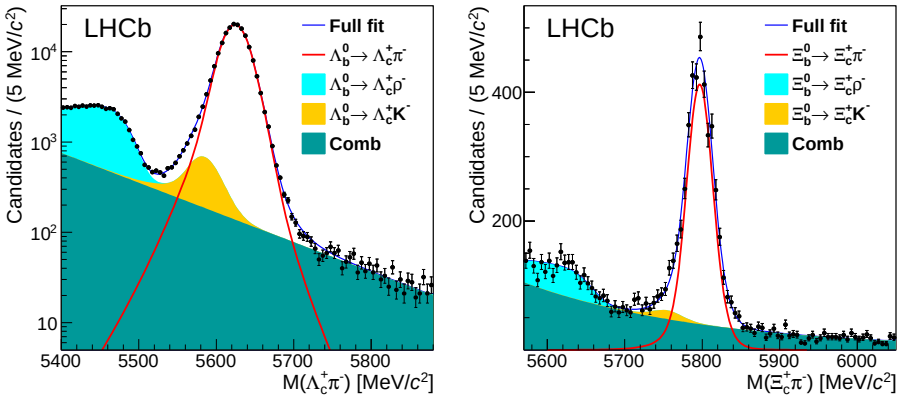

Figure 5: Fit to the b baryon invariant mass distribution for (left) Λ_b^0 and (right) Ξ_b^0 candidates. The data are black points and the fit components are described in the legend.

The ratio of lifetimes of the Ξ_b^0 and Λ_b^0 is measured by performing a fit with an exponential function to the efficiency corrected yield ratio in bins of decay time. This yields a ratio

$$\frac{\tau_{\Xi_b^0}}{\tau_{\Lambda_b^0}} = 1.006 \pm 0.018(\text{stat}) \pm 0.010(\text{syst})\,\text{ps}, \tag{1}$$

which can be further reduced using the known value of $\tau_{\Lambda_b^0}$ [15] to give

$$\tau_{\Xi_b^0} = 1.477 \pm 0.026(\text{stat}) \pm 0.014(\text{syst}) \pm 0.013(\tau_{\Lambda_b^0})\,\text{ps}. \tag{2}$$

These measurements are the most precise to date, and are consistent with predictions. This analysis demonstrates the potential of the LHCb dataset for doing high precision and high statistics studies of more b baryons in the future. For further details of this analysis please see Ref. [16].

5 Conclusions

The results of three recent LHCb analyses have been presented. They include two measurements that provide sensitivity to γ. The other result shows excellent progress in measuring the properties of the Ξ_b^0 baryon. These measurements give an indication of the power of the LHCb experiment to produce exciting results in the future using decays of b hadrons to open charm final states.

ACKNOWLEDGEMENTS

I thank the members of the LHCb collaboration for their help in preparing the talk and this document. Work supported by the European Research Council under FP7.

References

[1] M. Gronau and D. London, Phys. Lett. B **253** (1991) 483.

[2] M. Gronau and D. Wyler, Phys. Lett. B **265** (1991) 172.

[3] D. Atwood, I. Dunietz and A. Soni, Phys. Rev. Lett. **78** (1997) 3257 [hep-ph/9612433].

[4] A. Giri, Y. Grossman, A. Soffer and J. Zupan, Phys. Rev. D **68** (2003) 054018 [hep-ph/0303187].

[5] A. A. Alves, Jr. *et al.* [LHCb Collaboration], JINST **3** (2008) S08005.

[6] J. Insler *et al.* [CLEO Collaboration], Phys. Rev. D **85** (2012) 092016 [arXiv:1203.3804 [hep-ex]].

[7] T. Skwarnicki, DESY-F31-86-02.

[8] R. Aaij *et al.* [LHCb Collaboration], Phys. Lett. B **733** (2014) 36 [arXiv:1402.2982 [hep-ex]].

[9] R. Aaij *et al.* [LHCb Collaboration], Phys. Lett. B **726** (2013) 151 [arXiv:1305.2050 [hep-ex]].

[10] R. Aaij *et al.* [LHCb Collaboration], arXiv:1407.6211 [hep-ex].

[11] P. del Amo Sanchez *et al.* [BaBar Collaboration], Phys. Rev. Lett. **105** (2010) 081803 [arXiv:1004.5053 [hep-ex]].

[12] R. Aaij *et al.* [LHCb Collaboration], Phys. Lett. B **718** (2012) 43 [arXiv:1209.5869 [hep-ex]].

[13] J. Charles *et al.* [CKMfitter Group Collaboration], Eur. Phys. J. C **41** (2005) 1 [hep-ph/0406184].

[14] M. Bona *et al.* [UTfit Collaboration], JHEP **0803** (2008) 049 [arXiv:0707.0636 [hep-ph]].

[15] J. Beringer *et al.* [Particle Data Group Collaboration], Phys. Rev. D **86** (2012) 010001.

[16] R. Aaij *et al.* [LHCb Collaboration], Phys. Rev. Lett. **113** (2014) 032001 [arXiv:1405.7223 [hep-ex]].

[17] H. Albrecht *et al.* [ARGUS Collaboration], Phys. Lett. B **340** (1994) 217.